

# Status of the Correlation Process of the V-HAB Simulation with Ground Tests and ISS Telemetry Data

P. Plötner<sup>1</sup>, C. Roth<sup>2</sup>, A. Zhukov<sup>3</sup>  
*Technische Universität München, Garching, 85748, Germany*

M. Czupalla Ph.D.<sup>4</sup>  
*Kayser-Threde, München, 81379, Germany*

and

M. Anderson<sup>5</sup>, M. Ewert<sup>6</sup>  
*NASA Johnson Space Center, Houston, Texas 77058, USA*

**The Virtual Habitat (V-HAB) is a dynamic Life Support System (LSS) simulation, created for investigation of future human spaceflight missions. It provides the capability to optimize LSS during early design phases. The focal point of the paper is the correlation and validation of V-HAB against ground test and flight data. In order to utilize V-HAB to design an Environmental Control and Life Support System (ECLSS) it is important to know the accuracy of simulations, strengths and weaknesses. Therefore, simulations of real systems are essential. The modeling of the International Space Station (ISS) ECLSS in terms of single technologies as well as an integrated system and correlation against ground and flight test data is described. The results of the simulations make it possible to prove the approach taken by V-HAB.**

## Nomenclature

|                     |   |   |
|---------------------|---|---|
| <i>ARFTA</i>        | = | Advanced Recycle Filter Tank Assembly         |
| <i>ARS</i>          | = | Atmospheric Revitalization System             |
| <i>CCAA</i>         | = | Common Cabin Air Assembly                     |
| <i>CDRA</i>         | = | Carbon Dioxide Removal Assembly               |
| <i>ECLSS</i>        | = | Environmental Control and Life Support System |
| <i>IMV</i>          | = | Intermodular Ventilation                      |
| <i>ISS</i>          | = | International Space Station                   |
| <i>LSS</i>          | = | Life Support System                           |
| <i>MCL</i>          | = | Model Confidence Level                        |
| <i>OGA</i>          | = | Oxygen Generation Assembly                    |
| <i>P/C Module</i>   | = | Physio-Chemical Module                        |
| <i>RFTA</i>         | = | Recycle Filter Tank Assembly                  |
| <i>Sabatier CRA</i> | = | Sabatier Carbon Dioxide Reduction Assembly    |
| <i>SRV-K</i>        | = | Condensate Water Reclamation System           |
| <i>UPA</i>          | = | Urine Processing Assembly                     |
| <i>V-HAB</i>        | = | Virtual Habitat                               |
| <i>WCS</i>          | = | Waste Collection System                       |
| <i>WPA</i>          | = | Water Processing Assembly                     |
| <i>WRS</i>          | = | Water Recovery System                         |

<sup>1</sup> Student, Institute of Astronautics, Boltzmannstraße 15, 85748 Garching, Germany.

<sup>2</sup> Student, Institute of Astronautics, Boltzmannstraße 15, 85748 Garching, Germany.

<sup>3</sup> Ph.D. Student, Institute of Astronautics, Boltzmannstraße 15, 85748 Garching, Germany.

<sup>4</sup> Thermal Team Lead, Mechanical Analyses Department, Kayser-Threde GmbH, Perchtingerstr 5, 81379 Munich, Germany.

<sup>5</sup> Analysis Lead, Crew and Thermal Systems Division, 2101 NASA Parkway/EC211, Houston, TX, 77058

<sup>6</sup> Analysis Lead, Crew and Thermal Systems Division, 2101 NASA Parkway/EC211, Houston, TX, 77058

## I. Introduction

THE Virtual Habitat (V-HAB) is a dynamic Environmental Control and Life Support System (ECLSS) simulation. It makes a dynamic simulation of different LSS architectures for entire mission scenarios, including transfers between mission phases, possible, and allows access to such characteristics of the LSS as stability and controllability. V-HAB is a modular build program consisting of four parts<sup>1,2</sup>:

- a. Biological Module<sup>3</sup>
- b. Crew Module
- c. Physio-Chemical Module (P/C Module)
- d. Closed Environment Module<sup>4</sup>

An improvement of simulation accuracy is one of the major tasks in V-HAB development in order to increase the Model Confidence Level (MCL) of the modeling suite<sup>5</sup>. A correlation study of the V-HAB simulation with real ISS ECLSS data has been conducted to create a better representation of the ISS system. The simulation of the ISS ECLSS and its technologies results in major changes in the P/C Module. However, remaining program parts are not affected by these changes. The development and correlation of the ECLSS technologies as well as the ISS ECLSS are described in this paper. The presented study is the culmination phase of the V-HAB vs. ISS correlation activities reported in the past<sup>6,7</sup>.

## II. ISS ECLSS Technologies

The ECLSS technologies of the ISS can be divided in air revitalization and water recovery technologies. The air revitalization is handled by the following technologies. The carbon dioxide filtration is accomplished by the Carbon Dioxide Removal Assembly (CDRA) and Vozdukh. Oxygen is produced from water by the Oxygen Generation Assembly (OGA) and Elektron VM. The gathered carbon dioxide is reduced to water and methane by the Sabatier Carbon Dioxide Reduction Assembly (Sabatier CRA) with the help of hydrogen produced as a byproduct of the oxygen production. The temperature and humidity is controlled by the Common Cabin Air Assembly (CCAA). These technologies have to be taken into account for the simulations described following. There are several more systems but these concern trace contaminants, which are not simulated in V-HAB, and other aspects not as important for V-HAB.

The water recovery includes the urine processing by the Urine Processing Assembly (UPA) and the water processing, including processed urine, habitat condensate and others. Water is processed by the Water Processing Assembly (WPA) and the Condensate Water Reclamation System (SRV-K). A summary of all described technologies is shown in Table 1.

**Table 1. Simulated ISS ECLSS Technologies**

| Air Revitalization Technologies                           | Water Recovery Technologies                 |
|---|---|
| Carbon Dioxide Removal Assembly (CDRA)                    | Condensate Water Reclamation System (SRV-K) |
| Common Cabin Air Assembly (CCAA)                          | Urine Processing Assembly (UPA)             |
| Elektron VM   | Water Processing Assembly (WPA)             |
| Oxygen Generation Assembly (OGA)                          |   |
| Sabatier Carbon Dioxide Reduction Assembly (Sabatier CRA) |   |
| Vozdukh   |   |

## III. Models of the LSS Technologies

The previous described technologies are all built into V-HAB as models. As a description of all technologies would be too extensive for this paper, two examples are discussed. These examples are the CDRA and the Sabatier CRA. Further reading regarding the models of the other technologies can be found in the diploma thesis<sup>8</sup>.

## A. CDRA Model

The CDRA, seen in Figure 1, has two half cycle modes. The air enters from the CCAA, which implies that the air at the inlet is colder than the habitat temperature and contains less water vapor. With the first half cycle the air enters the upper desiccant bed, flows through the selector valve into the blower and precooler, followed by the lower adsorbent bed and through the lower desiccant bed to the air outlet. At the same time, the upper adsorbent bed is evacuated, first by the two stage pump to save air, and then to the accumulator tank of the Sabatier CRA.

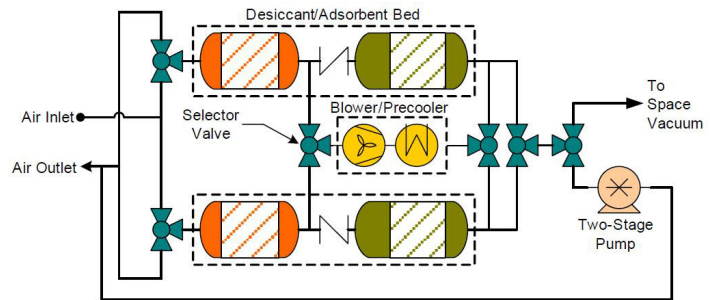


**Figure 1. Integration of the CDRA Components<sup>9</sup>**

During the last minutes of evacuation, the bed is exposed to space vacuum to vent residual  $\text{CO}_2$ . With the following half cycle, the air enters through the lower desiccant bed, thus the residual water vapor gets filtered as it would diminish the adsorbent efficiency. The air flow passes through the blower and precooler to the upper adsorbent bed, which has been evacuated before. It exits through the water loaded desiccant bed, which humidifies the air before leaving the CDRA. A half cycle takes 144 minutes on ISS<sup>10</sup>.

In V-HAB the thermal behavior of the adsorbent beds is accurately depicted by a dedicated thermal model of this sub-assembly, embedded in the previous existing CDRA model. The rate at which the  $\text{CO}_2$  is filtered matches the ground test data only at one partial pressure of  $\text{CO}_2$ . Furthermore, there is no physical model existing behind the adsorbent beds. The  $\text{CO}_2$  removal performance is independent from the simulated temperature and linearly dependent with the partial pressure of carbon dioxide.

With the test data<sup>11</sup> a temperature and pressure dependency was integrated into the newly created V-HAB CDRA model. The data points gathered by tests are connected by trend lines (seen as blue lines). A surface is approximated to match all trend lines as close as possible, resulting in the surface shown in Figure 2. The discontinuity in adsorb ability of the Zeolite around 800 Pa partial pressure of  $\text{CO}_2$  is due to a severe change in the test data. It does not have any influence on the CDRA performance during nominal operation, as the spacecraft maximum allowable concentration for durations of seven days or more is 7000 ppm<sup>12</sup>. This converts to about 710 Pa at international standard atmosphere sea level pressure. Therefore a concentration of more than 800 Pa is expected to be a rather exceptional case.

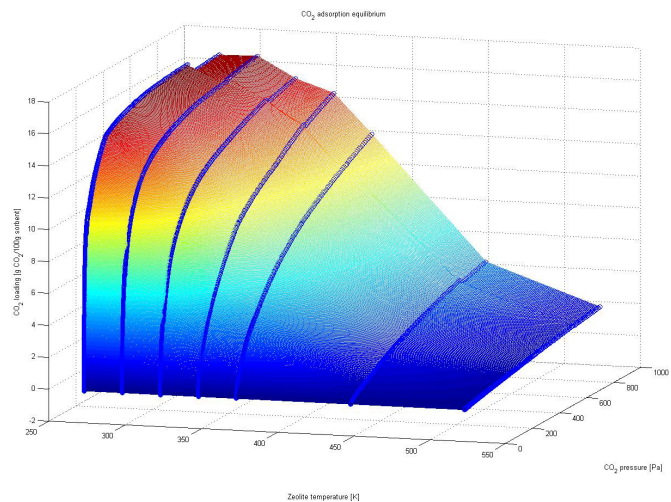


**Figure 2.  $\text{CO}_2$  adsorption of the Zeolite depending on the temperature and  $\text{CO}_2$  pressure**

The efficiency of CDRA was additionally updated with data obtained from performance tests<sup>10, 13</sup>. A detailed description of the physical and chemical processes of CDRA and the dependencies of the Zeolite can be found in a paper dedicated to the topic<sup>14</sup>.

With the Zeolite behavior (Figure 2) and the predicted bed temperature, the capacity of the sorbent beds is calculated with the current  $\text{CO}_2$  partial pressure (Figure 4). Figure 3 shows the improvement achieved with the updated CDRA V-HAB model, compared to the previously used simplified version. For the current simulation it is visible that with cooling of the sorbent beds the capacity rises. During the heated period however, the capacity is very close to zero, and zero during the bed exposure to space vacuum. The Zeolite  $\text{CO}_2$  partial pressure dependency can be seen in Figure 3 after about 45 hours as the  $\text{CO}_2$  injection rate is decreased, which results in a lowered  $\text{CO}_2$  partial pressure in the simulated habitat (Figure 4). Therewith, the sorbent bed capacity drops slightly. The capacity of the sorbent beds is important for the amount of absorbed  $\text{CO}_2$  and the velocity of absorption.

For a better evaluation of the results, the CO<sub>2</sub> partial pressure of the simulation is compared and correlated to the ISS CDRA Testing<sup>15</sup>. The data is only accessible in diagram form as shown in Figure 4. The simulation results are converted to torr (mmHg) and copied on top. The ground test is conducted at three different CO<sub>2</sub> injection rates equivalent to six (6 kg/day), four (4 kg/day) and three (3 kg/day) crewmembers. This shows a very good match of simulation and test results. The steady state values for the partial pressure match well. The dynamics in a single half cycle are also interesting.

Especially characteristic is the peak during each half cycle. An important variable to determine the partial pressure peak of CO<sub>2</sub> in the simulation is the test chamber volume. The chamber volume is assumed to be a perfect mixture in the simulation, which is not the case for a CO<sub>2</sub> concentration peak in the output of the CDRA. Therefore, the best match between simulation and reality is reached with a smaller simulated volume that correlates to the mixed volume in reality. The original test chamber is around 90 m<sup>3</sup>. Simulations with a chamber volume of 50 m<sup>3</sup> and 30 m<sup>3</sup> show more realistic peaks. However, the 30 m<sup>3</sup> chamber simulation has a nonlinear curve during the absorption process. Therewith, the 50 m<sup>3</sup> chamber seems to be the most accurate depiction of reality as shown in Figure 4. It is important to notice that the static partial pressure does not change with different chamber sizes.

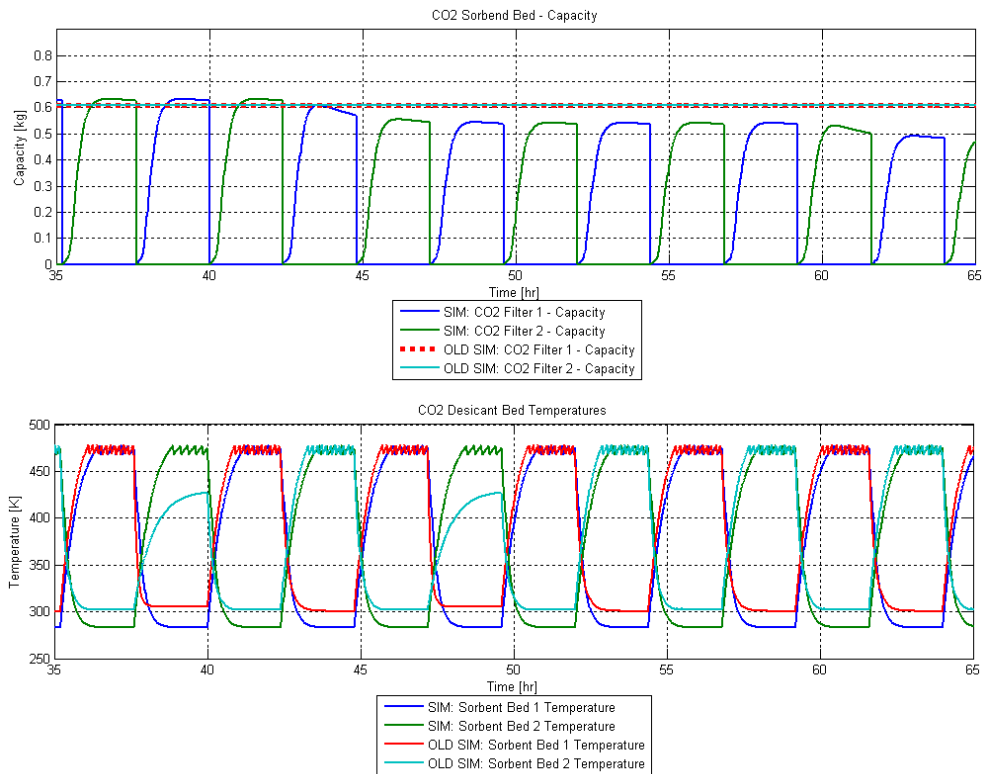


**Figure 3. CO<sub>2</sub> capacity of sorbent beds comparison of simulation and old simulation (top); temperature comparison of simulation and old simulation (bottom)**

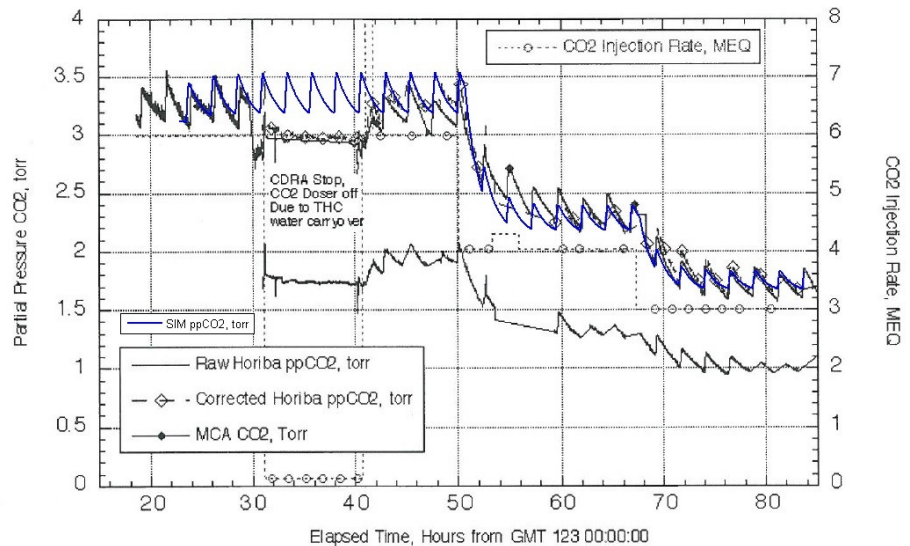


**Figure 4. Cabin CO<sub>2</sub> levels comparison of ground test (90 m<sup>3</sup>) and simulation (50 m<sup>3</sup>) (in torr)<sup>15</sup>**

It has to be noted that there is an average difference of 2.7 kg/hr between half cycle one and two in the ground test possible due to the interaction of the blower and the following selector valve<sup>15</sup>, therewith resulting in some irregularity. In the model the flow rates are assumed to be equivalent.

With on-orbit operations some changes have to be taken into account. The ISS orbits around the earth in 90 min. cycles with up to 37 min. of “night” and a minimum of 53 min. of day. During the “night” part, the ISS has to rely on battery power, which is recharged during the “day”. To minimize the battery power CDRA needs, power saving modes and strategies are discussed in a paper by Supra and Brasseaux in 1997<sup>16</sup>. These power saving efforts result in performance changes that have to be taken into account for the simulation of the ISS ECLSS if they are used.

### B. Sabatier CRA Model

The Sabatier CRA is built of two subsystems, the Carbon Dioxide Management Subsystem (CMS) and the Sabatier Reactor Subsystem (SRS). Both can be seen in Figure 5. The Sabatier CRA is fed by the CDRA and the Oxygen Generation Assembly (OGA). However, the production rates of these technologies are different and therewith one buffer tank is necessary to achieve optimal usage of CO<sub>2</sub> (filtered by CDRA) and H<sub>2</sub> (produced by OGA).

Therefore the CMS is installed. It consists of a piston compressor, which pumps the CO<sub>2</sub> from the CDRA adsorbent bed to the CO<sub>2</sub> accumulator tank, the second main component of the CMS.

The Sabatier reactor is part of the SRS and receives the H<sub>2</sub> directly from the OGA and the CO<sub>2</sub> from the accumulator tank.

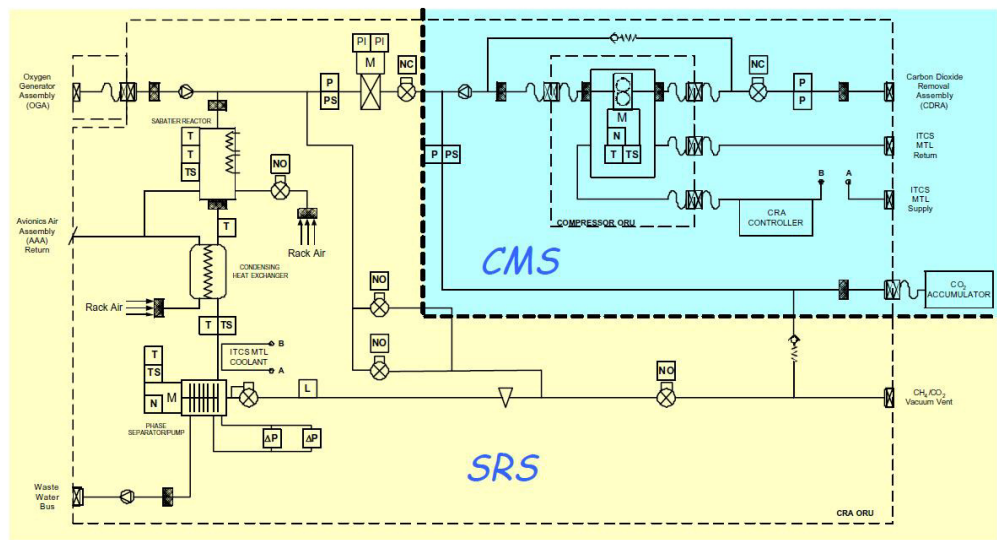


Figure 5. Sabatier Carbon Dioxide Reduction Assembly Schematic<sup>17</sup>

The reaction in the Sabatier reactor is dependent on a catalyst and the equilibrium conversion and reaction rate are dependent on temperature. A more detailed description, including an example of how to simulate the reactor, can be found in other references<sup>18</sup>. Downstream the reactor the gases flow through a condensing heat exchanger to condense the product water. A phase separator removes the water from the gases. The gases, mainly CH<sub>4</sub>, are vented into space. The product water is gathered and pumped into the WPA waste water tank.

The previous V-HAB Sabatier CRA model includes the Sabatier reactor and a condensing heat exchanger. These are sufficient components to run the Sabatier CRA stand-alone but not for an integrated simulation. Furthermore, a higher water production is predicted with the previous model. The water is continuously delivered to the WPA waste water tank.

In 2005 a 526 minutes long ground test of the Sabatier was conducted. The data gathered during this

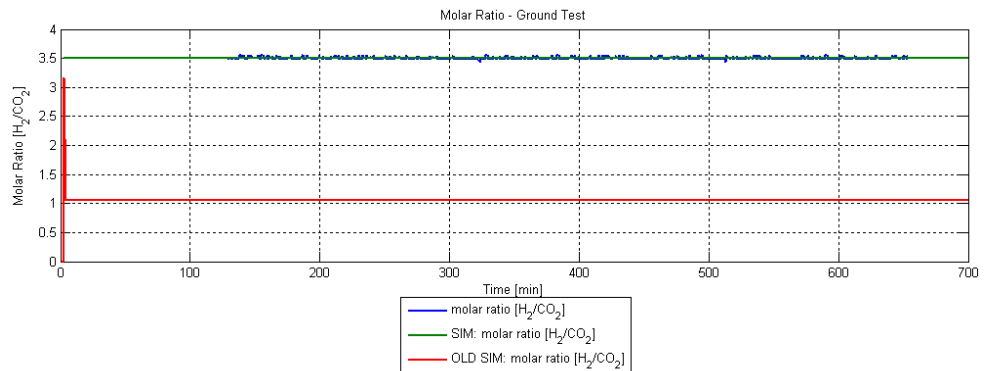


Figure 6. Molar ratio of input H<sub>2</sub> to CO<sub>2</sub> comparison of ground test, simulation and old simulation – constant ratio

test was the major reference for the correlation of the new V-HAB Sabatier model. Figure 6 shows the comparison of simulated molar ratios against the test data. The updated model results in a molar ratio of 3.5 mol H<sub>2</sub>/ mol CO<sub>2</sub> and coincides with the result of the ground test. This ratio is chosen due to production optimization analysis<sup>19</sup> and safety analysis<sup>20</sup>. The previous version of the Sabatier CRA model, however, has clearly a molar ratio around 1. This is important for the overall reaction efficiency and influences several processes discussed later. The peak seen at the beginning of the new simulation is due to a peak in the H<sub>2</sub> production of the OGA, which is explained in more detail in the diploma thesis<sup>8</sup>.

A comparison of the water production of both V-HAB Sabatier model versions against test data is shown in Figure 7. In the test data an offset of 126 minutes was incorporated to match the first water pump activation in the simulation to the ground test recorded data for better comparison. The water produced by the Sabatier CRA is not continuously pumped to the waste water tank. Therefore, another water accumulator tank is integrated with a pump,

which is activated when the water stored in the tank reaches a certain level. This can be seen as the small steps in Figure 7. To match the product water graph of the ground test, the amount of water in the waste water tanks has been reduced by approximately 1.5 kg ca. 490 minutes into the simulation. The difference between the Sabatier CRA versions can be seen in the continuous production of water as well as the roundabout doubled production of water in the older version.

The modeled efficiency as well as the amount and type of overboard vented substances are correlated against published test data<sup>19</sup>. Additional performance and exhaust data<sup>21</sup> has been used. The efficiency of the old version of the Sabatier CRA V-HAB model has no dependency on the molar ratio, which is shown in Figure 8. The new version has a smaller efficiency as well as a dependency on effects due to the molar ratio of H<sub>2</sub> and CO<sub>2</sub>. The minimum at a molar ratio of 4 is due to the decrease of the Sabatier reactor conversion efficiency if operated with a mixture near the stoichiometric ratio.

The decrease in efficiency further away from the stoichiometric ratio results from excess reactants vented over board, which carry product water with them. Therewith, two optimums for operation are present. The hydrogen rich optimum is not chosen due to higher risk of flammable gas leaking from the system or combusting in the system.

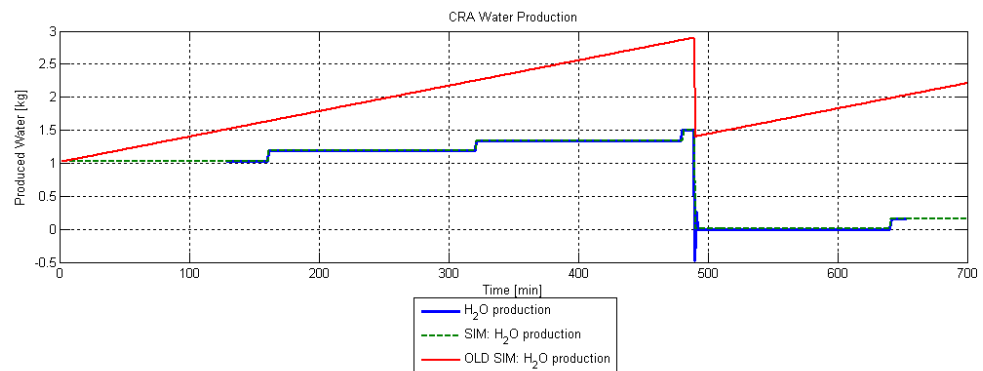


**Figure 7. Water production comparison of ground test, simulation and old simulation**

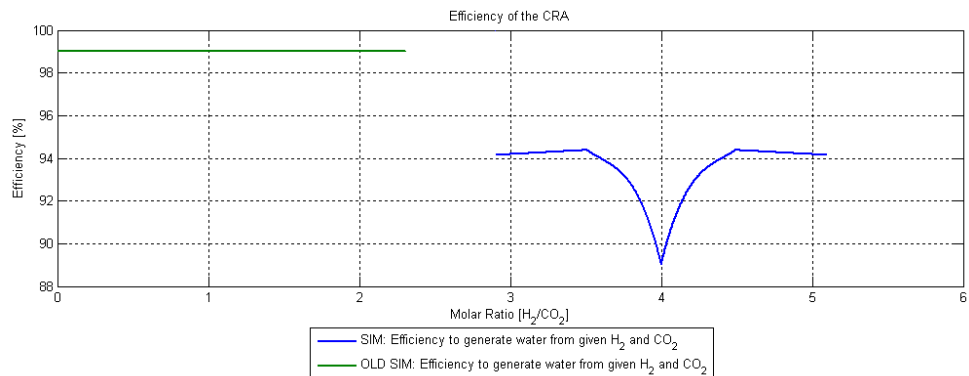


**Figure 8. Efficiency of converting the inputs (H<sub>2</sub> and CO<sub>2</sub>) into accumulated water compared between simulation and old simulation**

#### IV. Combined Test Cases for Correlation

In-between the simulation of each technology individually and the complete ECLSS of the ISS, an intermediate step was included to validate the interaction between several systems as well as the overall performance of the Atmospheric Revitalization System (ARS) and Water Recovery System (WRS).

### A. Atmospheric Revitalization System

Figure 10 shows the technologies (rectangles), tanks (boxes with rounded corners) and matter flows (arrows) programmed in V-HAB.

The OGA produces hydrogen for the Sabatier CRA. Based on analysis of flight data, its working mode was set to 30% of the maximum production rate. The unit is shut-off around two weeks before a resupply spacecraft docks to the ISS. The results for the oxygen production of the OGA are not different from the single test case and therewith, not discussed in particular.

The CCAA to dehumidify and cool the air before it reaches CDRA is not incorporated, as the CCAA is not part of the ARS rack. The input for the CDRA is simulated as if it would enter directly from the cabin. On ISS the CO<sub>2</sub> filtered by the CDRA is stored in the accumulation tank of the Sabatier CRA until a certain limit, and then excess CO<sub>2</sub> is vented overboard. This process is accomplished by an additional compressor between CDRA and Sabatier CRA, which is operated by specific rules<sup>22</sup>. In case there is not enough CO<sub>2</sub> the excess H<sub>2</sub> is vented overboard with all other gases. The water produced by the Sabatier CRA is pumped to the waste water tank when a certain amount is collected. The water has to be processed by the WPA before it is potable. All of this was depicted in the created ARS V-HAB model.

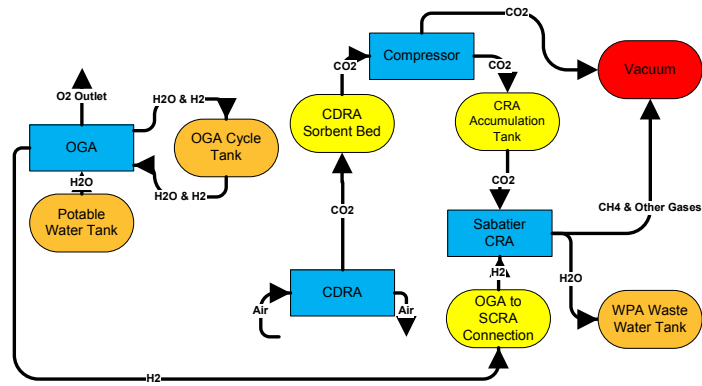


**Figure 10. Schematic of the Atmospheric Revitalization System implemented in V-HAB**

### B. Water Recovery System

The WRS is simulated separately to test V-HAB with fewer technologies before integrating the complete ISS ECLSS. The schematic of the system in V-HAB is shown in Figure 11. The UPA takes urine from the UPA waste water tank and recirculates it through the Advanced Recycle Filter Tank Assembly (ARFTA). Afterwards, the processed urine is delivered to the WPA waste water tank. Furthermore, the CCAA condenses water contained in the cabin air, which is pumped to the WPA waste water tank. Thereafter, the WPA filters the dirty water to produce drinkable water and deliver it to the potable water tank.

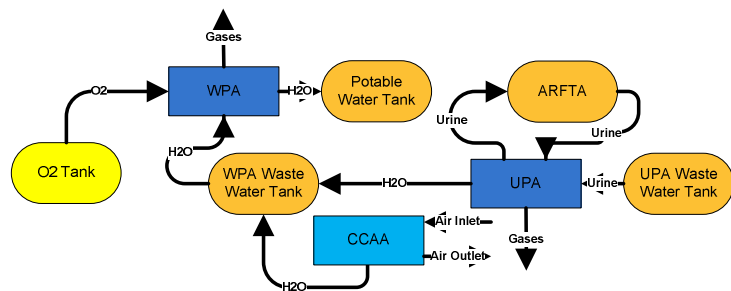


**Figure 11. Schematic of the Water Recovery System implemented in V-HAB**

Figure 12 shows the comparison of filling amounts in percent for three tanks. Knowing the tank size is helpful to get a better understanding of the results. The WPA waste water tank has a maximum capacity of 75 liters. However, 45.5 liters are considered the maximum to minimize fatigue. The potable water tank can contain up to 56.7 liters<sup>23</sup>. The UPA waste water tank can contain up to 12.9 liters. The UPA waste water tank is filled in steps, which on ISS results from the crew using the Waste Collection System (WCS)<sup>24</sup>. When the UPA waste water tank is filled to around 70% the UPA is activated. The first activation of the UPA is at a similar time in simulation and flight data. Due to longer breaks between filling the UPA waste water tank in the flight data, the UPA is activated earlier in the simulation. With the activation of the UPA the UPA waste water tank is emptied and at the same time the WPA waste water tank is filled. Due to the bigger tank, the filling level of the WPA waste water tank increases more slowly. Additionally, the condensate from the CCAA fills the tank. In the simulation the CCAA condenses more water, filling the WPA waste water tank faster than the one located on ISS. When the WPA waste water tank reaches a filling amount around 70% the WPA is activated, thereby emptying this tank and filling the WPA potable water tank. The water saved in the WPA potable water tank is mainly used for drinking and O<sub>2</sub> production. Beforehand it is filled in small containers resulting in the shown steps.

There are differences between the simulation and flight data. The simulation assumes identical loads and operations each day, while actual flight data includes variations due to individual crewmember metabolisms, scheduled activities, diet, and other factors each day. Given this difference in the inputs, the simulation and flight data seem to agree well.

## V. ISS ECLSS Simulation

In this stage of the ISS there are 16 pressurized parts consisting of 13 modules, one Soyuz spacecraft, a Pressurized Mating Adapter (PMA) and the Cupola. The result of the simulation volume calculation is a habitable volume of 378.33 m<sup>3</sup>, which was used for the V-HAB ISS model. The ISS was modeled as one big compartment at first and later as three compartments (see section VI). In addition, leakage is integrated in the V-HAB ISS model, which is calculated at a rate of 14.37 g/day during nominal operation on ISS.

### A. ISS Configuration

A schematic overview of the ISS and the modeled ECLSS technologies are shown in Figure 13. Not shown in this overview is the crew. Two human dummies are used each representing 1.5 crew members due to the 3 person crew during the simulated period. One dummy facilitates the Russian water recovery technologies, the other uses US systems. The values used for the human metabolism are partly taken from a medical reference<sup>25</sup>, which includes values for sleep, exercise and nominal situations. In fully closed V-HAB analyses, including the simulation of crew activities, this task shall be fulfilled by the V-HAB crew module, including the physiological human performance model<sup>26, 27</sup>. However, for the correlation of the P/C module this was not necessary. Furthermore, only one CCAA in the US Segment is condensing on ISS and the others only control the temperature. As the thermal solver, being a separate development<sup>28</sup>, was not integrated in V-HAB so far, the implementation of the remaining six CCAAs in the US Segment had not been necessary.

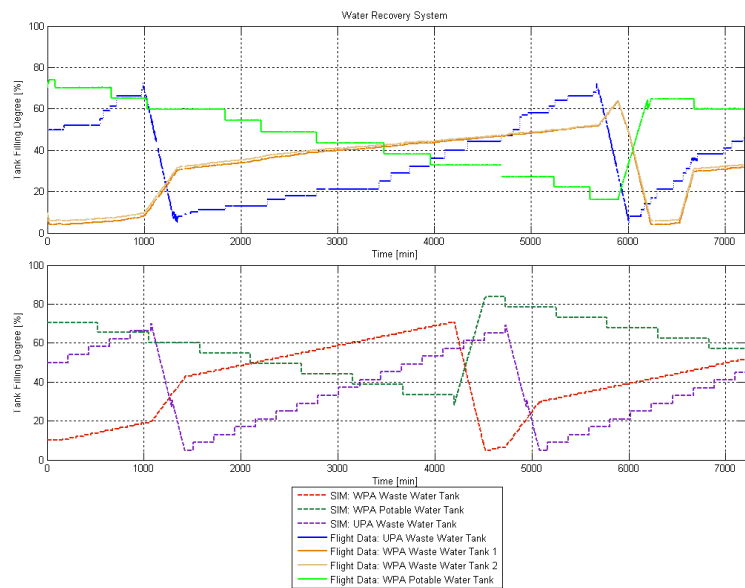


**Figure 12. Fill levels of UPA waste water tank, WPA waste water tank and potable water tank**

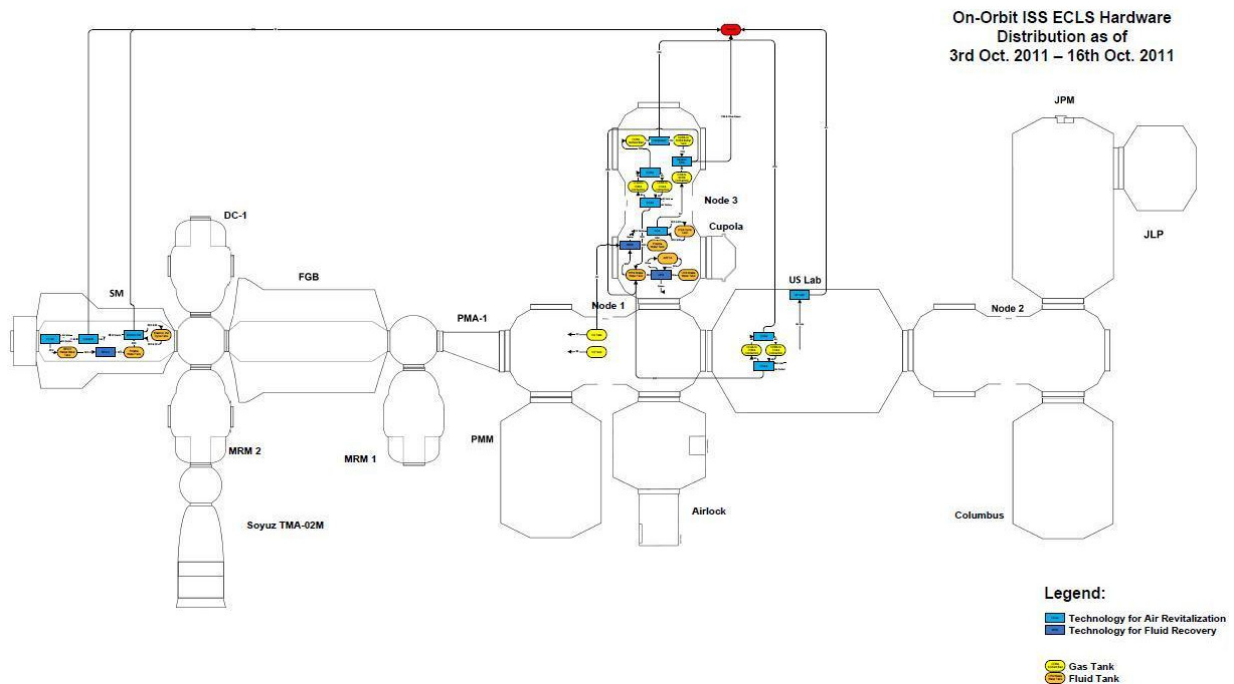


**Figure 13. Schematic overview of ISS ECLSS used for V-HAB, Oct. 3rd - Oct. 16th 2011**

**B. Comparison of Flight Data and Simulation Results - Atmosphere**

The time period, Oct. 3<sup>rd</sup> 2011 to Oct. 16<sup>th</sup> 2011, is used for the correlation of an ISS ECLSS V-HAB model to ISS telemetry data. It is chosen due to the fact that these 14 days have been particularly regular in regards to ECLSS operations. Furthermore, all simulated systems and sensors needed for correlation were running during this time period. Analysis of the simulation results start with the cabin air, for which the simulation results are shown in black.

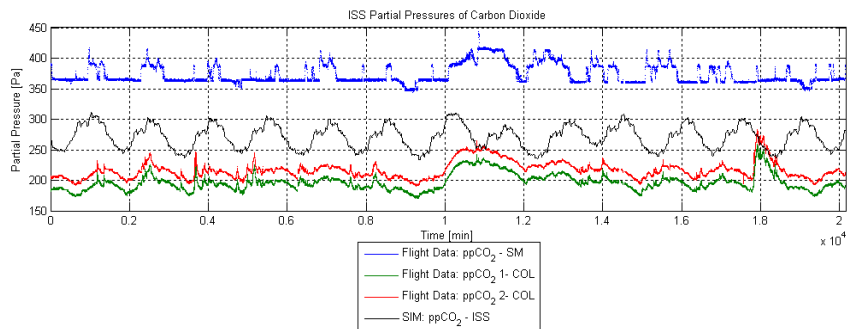


**Figure 14. CO<sub>2</sub> partial pressure comparison of simulation and ISS flight data**

The CO<sub>2</sub> partial pressure measured in the SM and Columbus is compared to the simulation results in Figure 14. It shows that the simulation prediction of CO<sub>2</sub> partial pressure is right in-between the sensor data from the ISS. The 24 hour cycle can be seen in the simulation results as well as flight data. During the day the CO<sub>2</sub> partial pressure rises slightly and is reduced in the night due to metabolic rate changes of the crew between night and day. The CDRA is not operable from minute 9892 to 10531. This results in an increased CO<sub>2</sub> partial pressure in this period and afterwards.

The differences between simulation and telemetry data can have several reasons. The compartment volume is a critical factor for the gradients of partial pressure. Assuming a slightly too small habitable volume will result in higher variations of the CO<sub>2</sub> partial pressure. Another possibility is the metabolism of the crew. Every human produces different amounts of CO<sub>2</sub><sup>25</sup>. Also, the schedule of the ISS crew is very dynamic and not documented to be easily incorporated in V-HAB. Therewith, it is difficult to know when, for how long and how intense it is exercised. Furthermore, the Vozdukh is modeled very close to the CDRA but might have significantly different performance in reality as there is not enough test data available for the Vozdukh.

The total pressure on ISS is decreasing for the first 16000 minutes as shown in Figure 15. Afterwards, it starts rising again. A first assumption was that this effect was caused by a leak and after reaching a minimum value, oxygen or nitrogen was added to the atmosphere. However, the real reason can only be seen if the partial pressures of CO<sub>2</sub> (Figure 14) and O<sub>2</sub> (Figure 16) are also taken into account.

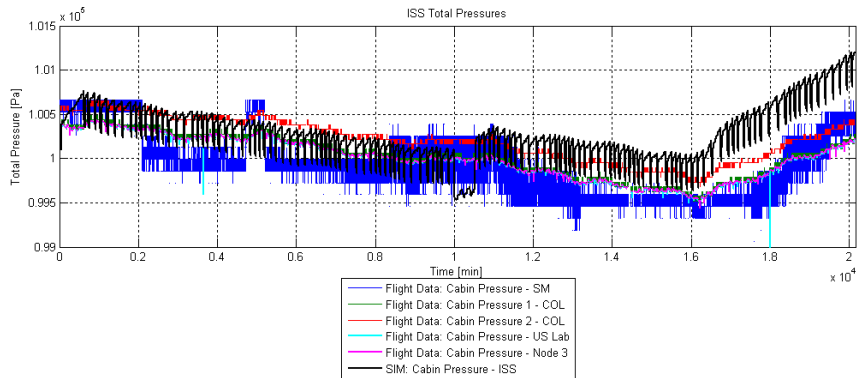


**Figure 15. Total pressure comparison of simulation and ISS flight data**

The partial pressure of CO<sub>2</sub> does not show the same tendency whereas the partial pressure of O<sub>2</sub> does show similar behavior as the total pressure. What happened is that the OGA at 30% production rate did not produce sufficient O<sub>2</sub> for a three person crew. Therewith, the partial pressure of O<sub>2</sub> decreased. After 16342 minutes the Elektron VM was activated. Thus, more O<sub>2</sub> was produced then consumed, which resulted in a partial pressure increase as well as total pressure increase.

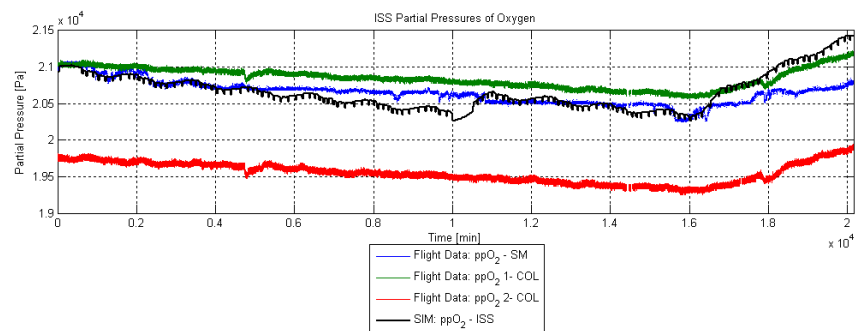
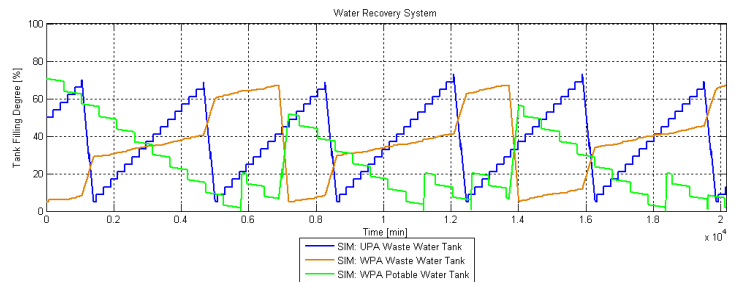


**Figure 16. O<sub>2</sub> partial pressure comparison of simulation and ISS flight data**

The 24 hour cycle is also seen in the simulated O<sub>2</sub> partial pressure. The telemetry data shows only very slight cycles if at all.

Possible reasons and resolutions for this have been mentioned already earlier for the high changes in CO<sub>2</sub> partial pressure. The oscillations in the simulated total pressure (Figure 16) are due to the continuous ON and OFF of the two CCAAs. This behavior is expected to be improved after the implementation of the newly developed thermal solver.



### C. Comparison of Flight Data and Simulation Results - Water

Figure 17 shows the simulation and telemetry data of the WRS tanks. The comparison starts with the UPA waste water tank. The flight data is clearly more irregular, which is not reasonable to simulate with exactly the same irregularity as the crew urination schedules were not recorded and cannot be depicted in the model precisely. In the shown data after about one week the Recycle Filter Tank Assembly (RFTA) is consumed, which leads to a different operation mode until it is replaced by a new one, in this case an

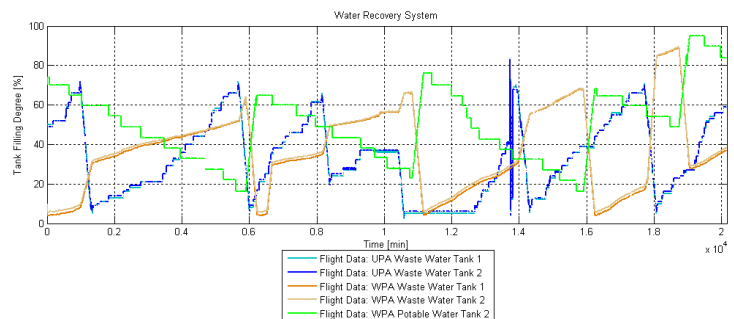


**Figure 17. Fill levels of UPA waste water tank, WPA waste water tank and potable water tank of the simulation (top) and ISS flight data (bottom)**

ARFTA. Compared to the flight data, the simulated data has a totally regular pattern. The average production rate of urine is matched accurate with six UPA cycles in the simulation and five cycles shown in the flight data with the UPA waste water tank filled to 60%.

For a more realistic simulation, the detailed human model of V-HAB could be implemented that would however require the depiction of precise drinking, eating and activity patterns of the crew, which are not recorded for the available ECLSS data time periods.

The graphs for the WPA waste water tank look generally similar. Differences are already incorporated due to the differences in the UPA waste water tank filling amount, resulting in different times of activation for the UPA. Moreover, the WPA on ISS is very likely turned ON manually, which results in changing maximum filling amounts. The ratio between WPA waste water tank increase and UPA waste water tank reduction seem to change. This seems odd as the UPA should generally convert 70% of the processed urine into waste water. A possible explanation is that stored water is added at this stage, which together with the activation of the WPA at a lower fill level would explain the difference between flight data and simulation.

The WPA potable water tank levels in the simulation and flight data look very similar. However, after 14 days there is a difference of 46.7 liters between simulation and flight data. One difference between simulation and operations on ISS is the tank that is supplied with additional water. Nominal 4.8 l/day water is resupplied from storage tanks on ISS<sup>23</sup>. How much of this water is resupplied on US or Russian side is not known. A major source for the inaccuracy of the amount of potable water is again the human dummy and the missing water usage data. Water consumption can change significantly between different crew members and crews. Baseline or planning rates are subject to change as well. The average water consumption per day for drinking, food preparation and personal hygiene for Expeditions 1 to 9 is 0.68 liters per person. The same average more than doubles to 1.38 liters per

person for Expedition 10<sup>29</sup>. In another source<sup>33</sup> this average is planned to be 2.2 liters per person-day for future missions. This shows the variability of the water consumption, in this case by a factor of 3. The flight data shows that all potable water is taken out with a certain step size. In the simulation, the OGA continuously uses water from the WPA potable water tank as this does not lead to an important difference in the simulation results.

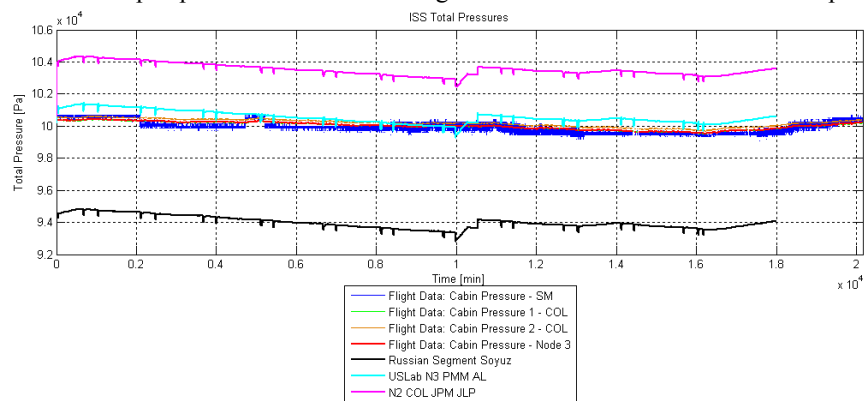


Figure 18. Total pressure comparison of simulation and ISS flight data

## VI. ISS ECLSS Simulation – Multiple Tanks

An interesting modification of the simulation model described earlier is the simulation of the habitable volume as multiple compartments. When multiple compartments are used, the atmosphere in each one can have a different composition. Furthermore, intermodular ventilation (IMV) is required. Values for the performance of the simulated IMV fans are taken from a paper dedicated to this topic<sup>30</sup>. To examine the sensitivity of the model to the number of compartments

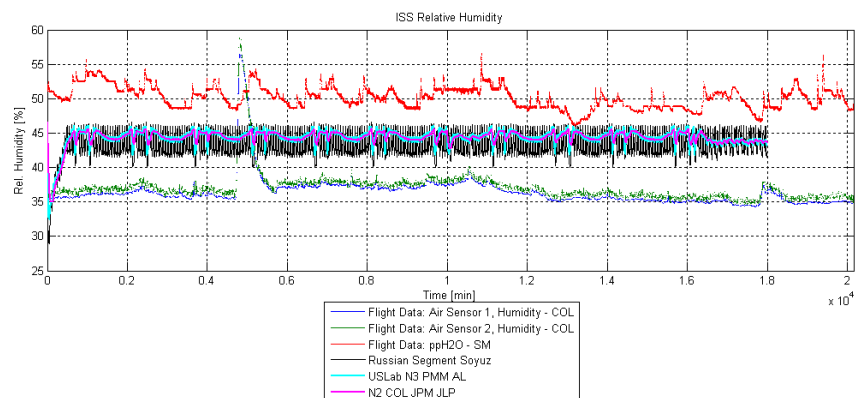


Figure 19. Relative humidity comparison of simulation and ISS flight data

assumed, the single habitable volume was divided into three compartments:

- a. Russian Segment and Soyuz
- b. US Laboratory, Node 1, Node 3, Permanent Multipurpose Module and Airlock
- c. Node 2, Columbus, Japanese Experiment Module

Parts of the results of this simulation are shown in Figure 18. However, a main problem for this type of simulation is the current solver used in V-HAB. The solver balances the pressure between connected compartments but afterwards, the IMV fans transport additional mass. This leads to total pressure offsets between the three compartments.

The relative humidity is shown in Figure 19 and at the same time shows one interesting effect of multiple compartments. Oscillations in one compartment are significantly smaller as in the following ones. The relative humidity in the Russian Segment clearly fluctuates with the highest and lowest extremes in the simulation.

## VII. Conclusion

V-HAB has seen major improvements during the past year. It has been possible to show that many existing expectations can be fulfilled with V-HAB. At least as important are the areas identified for improvement. Most of the work has been on the life support technology models of V-HAB. For CDRA, Sabatier CRA, OGA, WPA and UPA robust and precise models have been created. The Russian systems, Vozdukh, Elektron VM and SRV-K have models as close as possible to reality with the available data. With test data from these technologies a significant improvement of the ISS ECLSS model was possible. Finally, the CCAA has shown the necessity of a thermal solver for V-HAB. The CCAA model generally works but a significantly improved version is possible if air and coolant temperature changes can be taken into account.

The combination of the created technology models has been shown and therewith simulation of connected technologies (e.g. the ARS or WRS) is possible. This was necessary for the next step that has been made, the simulation of the ISS ECLSS. The previous most advanced V-HAB simulation of an existing ECLSS included two modeled technologies, Vozdukh and CDRA<sup>7</sup>. The ISS ECLSS model build for this work consists of nine different models for the different technologies, including improved models of the CDRA and Vozdukh. The previous simulation of the ISS has had a good fit of the CO<sub>2</sub> partial pressure between model and flight data. The current model fits CO<sub>2</sub> partial pressure, O<sub>2</sub> partial pressure, total pressure and the water recovery systems. The next step, a simulation with multiple compartments is only approximate so far, as it results in a significant delta of the total pressures between modules due to the IMV. This shall be improved as the thermal solver is being extended to become a thermal/fluid solver, which shall allow a continuous and precise IMV simulation.

Overall, with the precise depiction of state-of-the-art LSS technologies, and with the successful validation against on-ground test data (ARS, WRS) and flight data (ISS), V-HAB accomplished another leap towards a fully integrated mission simulation environment for spacecraft development.

## Acknowledgments

The V-HAB team is very grateful to the “Heinrich und Lotte Mühlfenzl-Stiftung“, which by providing Peter Plötner with a scholarship, made the visit and work at the NASA Johnson Space Center possible.

## References

- <sup>1</sup>Czapalla, Zhukov, A., Schnaitamm, J., Bickel, T., Walter, U., “The Virtual Habitat - A Tool for Dynamic Life Support System Simulations,” 40th International Conference on Environmental Systems, 2010-6016, 2010.
- <sup>2</sup>Czapalla, M., “The Virtual Habitat - Integral Modeling and Dynamic Simulation of Life Support Systems,” Verlag Dr.Hut, ISBN 978-3-8439-0305-9, 2011.
- <sup>3</sup>Czapalla, M., Zhukov, A., Mecsaci, A., Beck, M., Deiml, M., “Dynamic Life Support System Simulations with the Virtual Habitat,” 41st International Conference on Environmental Systems, 2011-5038, 2011.
- <sup>4</sup>Plötner, P., Czapalla, M., Zhukov, A., “Closed Environment Module - Modularization and Extension of the Virtual Habitat,” Advances in Space Research, submitted for publication.
- <sup>5</sup>Czapalla, M., Hager, P., Hein, A., Dirlich, T., Zhukov, A., Pfeiffer, M., “Model Confidence Level - A Systematic Metric for Development of a Virtual Space Habitat,” 39th International Conference on Environmental Systems, 2009-01-2514, 2009.

- <sup>6</sup>Zhukov, A., Czupalla, M., Stuffer, T., "Preparing the Correlation of the V-HAB Simulation with ANITA ISS Data," 40th International Conference on Environmental Systems, 2010-6123, 2010.
- <sup>7</sup>Zhukov, A., Czupalla, M., Knifka, M., Plötner, P., Stuffer, T., "Status of the correlation process of the V-HAB simulation with ANITA ISS data," 41th International Conference on Environmental Systems, 2011-5212, 2011.
- <sup>8</sup>Plötner, P., "Modeling of the ISS in V-HAB and Correlation with Flight and Ground Tests Data," Diploma Thesis, Technical University Munich, RT-DA-2012/20, 2012.
- <sup>9</sup>Yates, S.F., Kay, R.J., "High Capacity Adsorbent Development for Carbon Dioxide Removal System Efficiency Improvements," AIAA SPACE 2010 Conference & Exposition, AIAA 2010-8673, 2010.
- <sup>10</sup>Kay, R., "International Space Station (ISS) Carbon Dioxide Removal Assembly (CDRA) Protoflight Performance Testing," 28th International Conference on Environmental Systems, 981622, 1998.
- <sup>11</sup>Mulloth, L.M., Finn, J.E., "Carbon Dioxide Adsorption on a 5A Zeolite Designed for CO<sub>2</sub> Removal in Spacecraft Cabins," NASA, NASA/TM-1998-208752, 1998.
- <sup>12</sup>James, J., "Spacecraft Maximum Allowable Concentrations for Airborne Contaminants," Space Life Sciences Directorate, Lyndon B. Johnson Space Center, NASA, JSC-20584, 2008.
- <sup>13</sup>Knox, J.C., Howard, D.F., "Performance Enhancement, Power Reduction, and other Flight Concerns - Testing of the CO<sub>2</sub> Removal Assembly for ISS," 29th International Conference on Environmental Systems, 1999-01-2111, 1999.
- <sup>14</sup>Mohamadinejad, H., Knox, J.C., Smith, J.E., "Experimental and Numerical Investigation of Adsorption/ Desorption in Packed Sorption Beds under Ideal and Nonideal Flows," Separation Science and Technology, 35(1), pp. 1-22, 2000.
- <sup>15</sup>Knox, J.C., "International Space Station Carbon Dioxide Removal Assembly Testing," 30th International Conference on Environmental Systems, 2000-01-2345, 2000.
- <sup>16</sup>Supra, L.N., Brasseaux, S.F., "Molecular Sieve CO<sub>2</sub> Removal Systems: International Space Station and Lunar-Mars Life Support Test Project" 27th International Conference on Environmental Systems, 972419, 1997.
- <sup>17</sup>Murdoch, K., Perry, J., Smith, F., "Sabatier Engineering Development Unit," 33th International Conference on Environmental Systems, 2003-01-2496, 2003.
- <sup>18</sup>Anderson, M., "Sabatier Reactor ACM Model Report," Lockheed Martin Space Operations, MSAD-02-0476, 2002.
- <sup>19</sup>Murdoch, K. E., Allen G. F., "Parametric Impacts on Sabatier Water Production Capability," 29th International Conference on Environmental Systems, 1999-01-2121, 1999.
- <sup>20</sup>Jones, H. W., "Safety Analysis of Carbon Dioxide Reduction Technologies," 41th International Conference on Environmental System, AIAA 2011-5216, 2011.
- <sup>21</sup>Abney, M., Miller, L., Williams, T., "Sabatier Reactor System Integration with Microwave Plasma Methane Pyrolysis Post-Processor for Closed-Loop Hydrogen Recovery," American Institute of Aeronautics and Astronautics, M10-0219 M10-0457, 2010.
- <sup>22</sup>Jeng, F., "Status of Analysis Support to the Integrated Sabatier EDU Test, Rev. A.," Lockheed Martin Space Operations, MSAD-04-0286, 2005.
- <sup>23</sup>Yeoman, D. A., Shkedi, B., Tobias, B., "International Space Station Water System Architecture and Operational Plan," 38th International Conference on Environmental Systems, 2008-01-2007, 2008.
- <sup>24</sup>Lee Broyan, Jr. J., "Waste Collector System Technology Comparisons for Constellation Applications," 37th International Conference on Environmental System, 2007-01-3227, 2007.
- <sup>25</sup>Guyton, M.D. A. C., "Textbook of Medical Physiology," W. B. Saunders Company, ISBN 0-7216-1260-1, 1986.
- <sup>26</sup>Zhukov, A., Czupalla, M., Stuffer, T., "Preparing the Correlation of the V-HAB Simulation with ANITA ISS Data," 40th International Conference on Environmental Systems, 2010-6123, 2010.
- <sup>27</sup>Zhukov, A., Czupalla, M., Stuffer, T., "Preparing the Correlation of the V-HAB Simulation with ANITA ISS Data," 40th International Conference on Environmental Systems, 2010-6123, 2010.
- <sup>28</sup>Zhukov, A., Roth, C., Plötner, P., Czupalla, M., "Simulation of the Temperature and Humidity Control System of International Space Station in the Virtual Habitat," 43rd International Conference on Environmental Systems, submitted for publication.
- <sup>29</sup>Bobe, L. S., Samsonov, N. M., Soloukhin, V. A., Farafonov, N. S., Novikov, V. M., Andreichuk, P. O., Protasov, N. N., Romanov, S. Ju., Sinyak, Ju. E., Skuratov, V. M., "Water Supply of the Crew of a Space Station Through Water Recovery and Water Delivery: SRV-K and SPK-U System Operation on ISS," 35th International Conference on Environmental Systems, 2005-01-2806, 2005.
- <sup>30</sup>Son, C. H., Smirnov, E. M., Ivanov, N. G., Telnov, D. S., "Integrated Computational Fluid Dynamics Ventilation Model for the International Space Station," 35th International Conference on Environmental System, 2005-01-2794, 2005.